Eur. Phys. J. B **42**, 503–508 (2004)
DOI: 10.1140/epjb/e2005-00009-7

THE EUROPEAN PHYSICAL JOURNAL B

# Electronic structure in finite-length deformed metallic carbon nanotubes

Hui Jiang[1,2,a], Wei Bu[1], Jie Jiang[1], and Jinming Dong[1]

[1] Department of Physics and National Laboratory of Solid State Microstructures, Nanjing University, 210093 Nanjing, P.R. China
[2] Department of Mathematics and Science, Huaihai Institute of Technology, Lianyungang, 222005 Jiangsu, P.R. China

Received 9 April 2004 / Received in final form 7 November 2004
Published online 18 January 2005 – 

**Abstract.** Using the $\pi$-band tight-binding (TB) model and the quantum box boundary condition, we have discussed how both of the applied strain and finite-length affect the energy bands of metallic carbon nanotubes (CNTs). It is found that, for finite-length CNTs, energy gap for the armchair tube under uniaxial strain and metallic zigzag tube under torsional strain will oscillate with increasing strain, which do not exist in the case of infinite-length CNTs, and will be able to be observed by experiments in future.

**PACS.** 71.20.Tx Fullerenes and related materials; intercalation compounds

## 1 Introduction

Since their discovery [1] in 1991 by Iijima, the carbon nanotubes (CNTs) have been of great interest in mesoscopic physics and nanotechnology because of their unique physical and chemical properties [2]. Theoretical studies predicted that a carbon nanotube can be either metallic or semiconducting, depending on its helicity and size [3,4], which has been confirmed by experimental observations, e.g. the scanning tunneling microscopy (STM) studies on the single-walled carbon nanotubes (SWNTs) [5,6].

Nanotubes, however, are usually supported on a solid substrate in the experiments, causing various mechanical deformations of the CNTs, and corresponding changes of their electronic structures, shown by the atomic force microscopy and molecular mechanics calculations [7,8]. For example, a symmetry breaking due to the deformation may remove the energy level degeneracy. An increased curvature due to the deformation can enhance the $\sigma$-$\pi$ mixing and rehybridization. Experimentally, resistance of SWNT transistors was found to vary significantly under bending and stretching [9], and an observed torsion of a metallic SWNT was speculated to open a small band gap [10]. Several theoretical studies on the $\pi$-electronic properties of the deformed SWNTs under two kinds of strains, i.e. the uniaxial and torsional [11–15], have shown that the band structures of the deformed SWNTs are determined by their chiral symmetries and the kind of strains. Most of the deformed SWNTs show a metal-semiconductor transition, occuring repeatedly with increasing strain. It is known that under uniaxial strain, the derivative of band gap over strain is the largest for zigzag tubes and decreases with increasing the chiral angle. In contrast, under torsional strain, the derivative becomes the largest for armchair tubes and decreases with decreasing the chiral angle. In particular, armchair tubes under uniaxial strain and metallic zigzag tubes under torsional strain remain to be metallic [14,15].

Some recent progresses in research of the CNTs show that they can be cut into short segments in length of a few tens of nanometers [16]. In general, limiting CNT length will lead to new electronic properties of CNTs. Moreover, CNTs in practical experiments have only finite-length. Thus, it is important to study such quantum size effects in real systems. Actually, the discrete energy levels due to finite-length of individual nanotubes and ropes were observed in transport experiments [17,18]. Theoretically, the energy levels of finite-length CNTs were found to be tailored by the length and diameter of the nanotube [19] and the standing-wave (SW) was observed [20]. Due to the finite-length effects, the energy band of infinite-length nanotubes will become the discrete energy levels in finite-length nanotubes, making the finite-length CNTs to be semiconducting even they are metallic in the case of infinite-length.

In fact, it is inevitable to have both strains and finite-length effects in the actual applications of CNTs. So, it is interesting and important to study how coexistence of the strain and finite-length affects electronic properties of CNTs. In this paper, using the $\pi$-band tight-binding (TB) model and the quantum box boundary condition, we discuss this problem in two kinds of deformed metallic nanotubes, i.e. the armchair under uniaxial strain and the metallic zigzag tube under torsional

[a] e-mail: jhui_xm@hotmail.com

strain. The $\sigma - \pi$ hybridization effect [21,22], which is particularly important for CNTs with small diameter, is not included in our TB based calculations.

This paper is organized as follows. In Section 2, the electronic property of the finite-length deformed SWNTs are presented. Results and discussions are given in Section 3.

## 2 Method

A SWNT can be defined by a two-dimensional (2D) lattice vector, $\vec{R} = n\vec{a}_1 + m\vec{a}_2$ with $\vec{a}_1$, $\vec{a}_2$, the 2D unit vectors of graphene sheet and $(n, m)$, a pair of integers (Fig. 1). $c_h = \sqrt{n^2 + nm + m^2}$, is the circumference of the tube in a unit of the equilibrium lattice constant, $\left|\vec{a}_1\right| = \left|\vec{a}_2\right| = a_0$.

By using the nearest neighbor $\pi$-band TB model with one orbital per atom, the Hamiltonian of a deformed nanotube $(n, m)$ can be given by:

$$H'_T = \sum_{\langle i,j \rangle} \left\{ t_{i,j} c_i^+ c_j + \text{h.c.} \right\}. \tag{1}$$

Here, the sum over $i, j$ is restricted to the nearest-neighbor sites. The hopping coefficients $t_{i,j}$ are taken to be three deferent values of $t_1, t_2, t_3$ for three kinds of deformed c-c bonds $(r_1, r_2, r_3)$, shown in Figure 1. Neglecting the curvature effect, the primary effect of the bond deformation is to alter the hopping parameters between the two nearest neighbor carbon atoms, which is assumed to scale with the bondlength as $t_i = t_0(r_0/r_i)^2 (i = 1, 2, 3)$ with $t_0$ ($t_0 = -2.7$ eV) and $r_0$, the hopping parameter and bond length of the undistorted tube, respectively [23]. Three $t_i$ $(i = 1, 2, 3)$ are given as follows:

$$\begin{aligned}
t_1 &= t_0 4c_h^2 \Big( \left[ \sqrt{3}(n+m)(1+e_c) - (n-m)\tan(\gamma) \right]^2 \\
&\quad + (n-m)^2 (1+e_t)^2 \Big)^{-1}, \\
t_2 &= t_0 4c_h^2 \Big( \left[ -\sqrt{3}m(1+e_c) + (2n+m)\tan(\gamma) \right]^2 \\
&\quad + (2n+m)^2 (1+e_t)^2 \Big)^{-1}, \\
t_3 &= t_0 4c_h^2 \Big( \left[ -\sqrt{3}n(1+e_c) - (n+2m)\tan(\gamma) \right]^2 \\
&\quad + (n+2m)^2 (1+e_t)^2 \Big)^{-1}.
\end{aligned} \tag{2}$$

Here, $e_t$ and $e_c$ represent the strains along the tube axis and circumference, respectively, in the case of uniaxial strain. And the Poisson ratio $\sigma$ is equal to 0.2 (i.e. $e_c = -0.2e_t$) [15]. $\gamma$ is the shear strain. Then, diagonalization of the Hamiltonian $H'_T$ gives an 1D band structure of the nanotube $(n, m)$ [14]

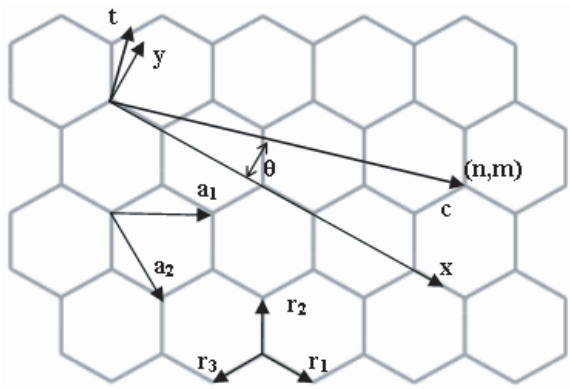


**Fig. 1.** Structure of a single graphene sheet. $r_1$, $r_2$ and $r_3$ correspond to bond 1, 2, and 3, respectively. $\vec{a}_1$ and $\vec{a}_2$ are the lattice vectors of the two dimensional sheet. $\hat{c}$ and $\hat{t}$ are unit vectors along the circumference and tube axis, respectively.

$$\begin{aligned}
E_\pm(N,k) = \pm\Big\{ & t_1^2 + t_2^2 + t_3^2 \\
& + 2t_1t_2 \cos\Big( \pi N \frac{n+2m}{c_h^2} - \frac{\sqrt{3}}{2}\frac{n}{c_h} k (1+e_t) a_0 \\
& - \pi N \frac{\sqrt{3}\tan(\gamma)}{1+e_c}\frac{n}{c_h^2} \Big) \\
& + 2t_1t_3 \cos\Big( \pi N \frac{2n+m}{c_h^2} + \frac{\sqrt{3}}{2}\frac{m}{c_h} k (1+e_t) a_0 \\
& + \pi N \frac{\sqrt{3}\tan(\gamma)}{1+e_c}\frac{m}{c_h^2} \Big) \\
& + 2t_2t_3 \cos\Big( \pi N \frac{n-m}{c_h^2} + \frac{\sqrt{3}}{2}\frac{n+m}{c_h} k (1+e_t) a_0 \\
& + \pi N \frac{\sqrt{3}\tan(\gamma)}{1+e_c}\frac{n+m}{c_h^2} \Big) \Big\}^{\frac{1}{2}},
\end{aligned} \tag{3}$$

where, $N = 1, ..., N_c$ ($N_c$ is the hexagon number in an 1D unit cell), and $-\frac{\pi}{T} \le k \le \frac{\pi}{T}$ ($k$ is the wave vector along the tube axis) with $T$, the deformed 1D lattice constant determined by $T = (1+e_t)\sqrt{3}c_h a_0 / gcd(2n+m, n+2m) = (1+e_t)T_0$. Here, gcd refers to the largest common divisor and $T_0$ is the periodicity of undeformed CNT. The plus and minus subscripts in equation (3) stand for the conduction and valence band, respectively. The band gap of a $(n, m)$ tube in the presence of uniaxial ($\gamma = 0$) or torsional strain ($e_c = e_t = 0$) can be easily calculated from equation (3).

In case of armchair tubes $(n, n)$ under uniaxial strain, the energy dispersion relationship around the Fermi level

can be obtained from equation (3) with $N = n$,

$$E_{\pm}(k) = \pm\Bigg\{t_1^2 + 2t_2^2 - 4t_1t_2\cos\left(\frac{1}{2}k(1+e_t)a_0\right) + 2t_2^2\cos\left(k(1+e_t)a_0\right)\Bigg\}^{\frac{1}{2}}. \quad (4)$$

By setting $E_{\pm}(k) = 0$, we can find that the new Fermi wave vector is now determined by $k_F = \pm\frac{2}{T}\arccos\left(\frac{t_1}{2t_2}\right)$, which will change with the applied strain $e_t$. Obviously, if the uniaxial strain disappears, we can still obtain $k_F = \pm\frac{2\pi}{3T_0}$. Because the Fermi level of armchair tubes under the uniaxial strain is still set to be zero, $E_{\pm}(k)$ can be expanded over the small $\Delta k = k - k_F$ and an approximated expression is obtained as follows,

$$E_{\pm}(k) \approx \pm\frac{T}{2}\sqrt{4t_2^2 - t_1^2}\Delta k, \quad (5)$$

which can be regarded as two lines (1, 2) through $k_{f1}$ and two lines (3, 4) through $k_{f2}$, with $k_{f1} = \frac{2}{T}\arccos\left(\frac{t_1}{2t_2}\right)$ and $k_{f2} = -\frac{2}{T}\arccos\left(\frac{t_1}{2t_2}\right)$.

The metallic zigzag tubes $(n, 0)$ under torsional strain have two metallic subbands ($N = \frac{2n}{3}, \frac{4n}{3}$) around the Fermi level. Similar to the armchair tubes under the uniaxial strain, we can obtain the dispersion relationship around the Fermi level by expanding $E_{\pm}(k)$ at $k_F$,

$$E_{\pm}(k) \approx \pm\frac{T_0}{2}t_2\Delta k. \quad (6)$$

with the Fermi wave vector $k_F = \pm\frac{2}{T_0}(\frac{2\pi}{3} - \arccos(-(t_1 - \frac{1}{2}t_3)/t_2))$. It is apparent that the energy dispersion relation around the Fermi level can also be regarded as four lines, which are in fact double-degenerate for a perfect metallic zigzag tube with $k_F = 0$. However, in contrast to the case of armchair tubes under the uniaxial strain, two Fermi wave vectors of metallic zigzag tubes under torsional strain belong to the different metallic subband ($N = \frac{2n}{3}, \frac{4n}{3}$), respectively.

Now, we transfer our attention to the finite-length effect. In the simple 1D quantum box model, the electron eigenstates are SW of the form $\sin(kx)$. So, we can obtain $kL = j\pi$, with $j = 0, 1, \cdots$, $0 \le k < \pi/T$. Here, $L = (l+1)T/2$ is the effective tube length and $l$ is the total atomic layer number along the tube axis [20]. Then, the discontinuous wave vector can be obtained as

$$k = \frac{2\pi j}{(l+1)T_0(1+e_t)}; \quad \text{(uniaxial)} \quad (7a)$$

$$k = \frac{2\pi j}{(l+1)T_0}. \quad \text{(torsional)} \quad (7b)$$

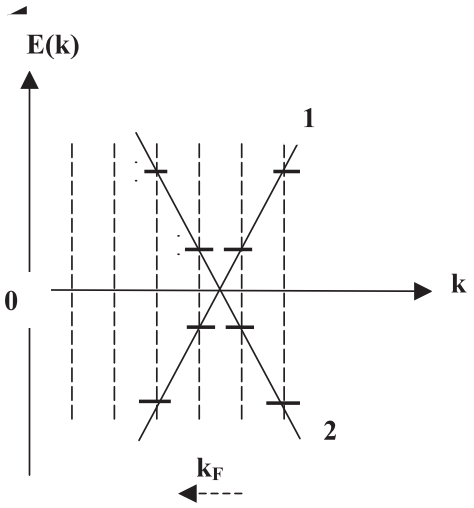


**Fig. 2.** Energy dispersion relationship around Fermi level of armchair tube. The lines 1 and 2 represent the two allowed bands. Arrowheads represent the movement direction of Fermi wave vector. Broken lines represent the discrete allowed wave vector, and short transverse lines represent allowed discrete energy levels.

Considering the quantized wave vector $k$, equations (5) and (6) can be expanded as follows:

$$E_{gap} = T\sqrt{4t_2^2 - t_1^2}\min\left(\left|\frac{2\pi j}{(l+1)T} - k_F\right|\right), \text{ (armchair)} \quad (8)$$

$$E_{gap} = T_0|t_2|\min\left(\left|\frac{2\pi j}{(l+1)T_0} - k_F\right|\right), \quad \text{(zigzag)} \quad (9)$$

where $\min(\cdots)$ represents choice of the minimal value of the expression in the bracket.

## 3 Results and discussion

Because there are two variables, i.e. the applied strain and tube length, in the energy-gap expression of these two kinds of finite-length deformed metallic CNTs, we divide our discussion into two parts.

First of all, we study the case of the fixed finite-length tubes with increasing applied strain. Firstly, we consider the armchair CNTs under uniaxial strain. By using equation (2), the hopping coefficients for the three kinds of deformed $c-c$ bonds is obtained as: $t_1 = t_0(1-2e_c)$ and $t_2 = t_3 = t_0[1-(e_c+3e_t)/2]$. And equation (8) can be reduced to

$$E_{gap} = \sqrt{3}|t_0|(1-2e_t)T\min\left(\left|\frac{2\pi j}{(l+1)T} - k_F\right|\right), \quad (10)$$

with $k_F = \frac{2}{T}\arccos\left(\frac{1}{2} + 0.9e_t\right) \approx \frac{2\pi}{3T}(1-e_t)$. With increasing strain $e_t$, $k_F$ holds allowed wave vector or not, alternatively, implying that a phase transition between metal and semiconductor will take place (Fig. 2). According to equation (10) and fix $l = 98$, we can get the relationship between energy gap and strain, and the obtained

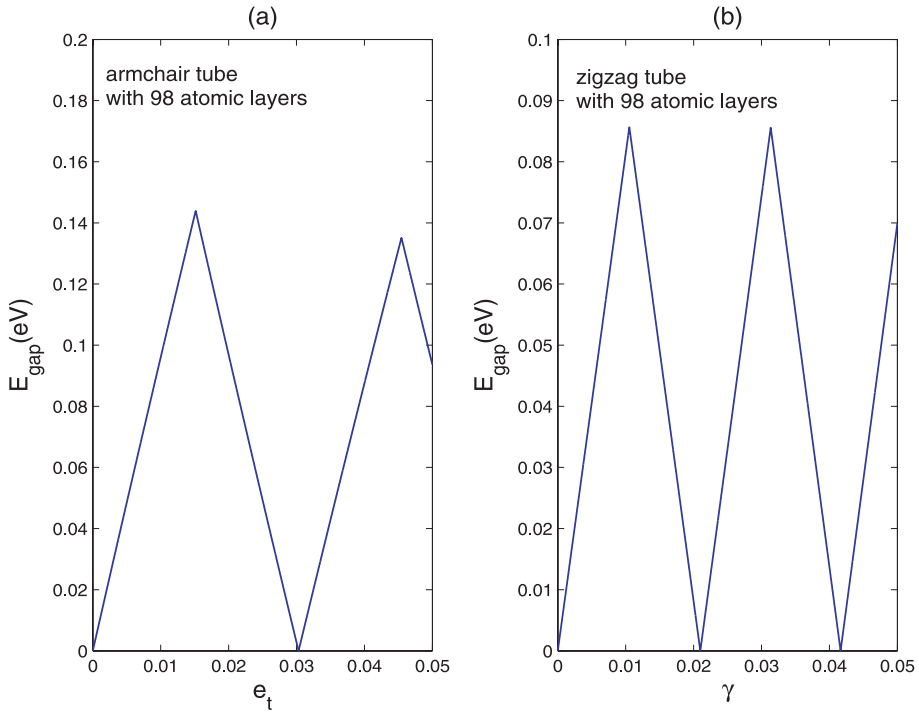


**Fig. 3.** Energy gap versus strain for finite-length armchair tube under uniaxial strain (a) and metallic zigzag tubes under torsional strain (b). The energy gaps of these two kinds of infinite-length deformed tubes will equal to zero, which is independent of the applied strain.

result is shown in Figure 3a, from which the periodic oscillation of energy gap can be observed. Using the analytical method, we find the oscillation period equals to $3/(l+1)$, which will decrease with increasing the tube length. Obviously, if $l =$ infinite, the periodic oscillation of the energy gap will vanish. It is also found that there is a maximal value of energy gap in each period, whose corresponding Fermi wave vector lies between two nearest discrete allowed wave vectors. Moreover, with increasing $e_t$, the maximal value of energy gap in each period will gradually decrease, which is due to the absolute value of the slope of $E_{\pm}(k)$ around the Fermi level decreases with increasing the strain, causing the corresponding decrease of the energy gap. Secondly, we turn to the case of fixed finite-length metallic zigzag tubes under the torsional strain by using the same way as stated above. According to equation (2), equation (9) can be reduced to,

$$E_{gap} = T_0 \left|t_0\right| \left(1-\gamma^2\right) \min\left(\left|\frac{2\pi j}{T_0\left(l+1\right)} - k_F\right|\right), \quad (11)$$

with $k_F = \frac{2}{T_0}\left(\arccos\left(-\left(\frac{1}{2}+\frac{3\sqrt{3}}{4}\gamma\right)\right) - \frac{2\pi}{3}\right) \approx \frac{2}{T_0}\left(1.5\gamma+\gamma^2/\sqrt{3}\right)$. The periodic oscillation of the energy gap can still be observed (shown in Fig. 3b). And the analytical expression of the oscillation period is approximately obtained as $\pi/\left(1.5\times(l+1)\right)$, which will decrease with increasing the tube length. However, with increasing the strain $\gamma$, the maximal value of energy gap in each period almost does not change, which is due to very small $\gamma^2$ in equation (11). In a word, when the atomic layer number is fixed, the energy gaps of these two kinds of deformed metallic nanotubes will oscillate periodically with increasing of the strain.

Finally, we study the energy gap of deformed CNTs under fixed strain with increasing tube length and still obtain the periodic oscillation of the energy gap. First, we take the elongated armchair tube ($e_t = 0.03$) as an example. The result of energy gap versus tube length is shown in Figure 4. With the help of equation (10), using the analytical perturbation method, we find there are two fundamental oscillation frequencies, i.e. a slow one at $e_t$ and a fast one at $(1-e_t)/3$, which can be exactly found from their Fourier Frequency Analysis (FFA) (shown in Fig. 5). And it is apparent that the slow and fast oscillation frequencies will increase and decrease, respectively, with increasing the strain. Furthermore, it can be found in Figure 4 that the maximums of energy gap in each period decrease with increasing of tube length. This is because the difference between two nearest discrete allowed wave vectors $k$ will become smaller when the tube length is increased. Obviously, if the tube is infinite, the wave vector $k$ will be continuous, leading to zero energy-gap. For the twisted metallic zigzag tube ($\gamma = 0.03$), similar conclusion can be drawn and the related result is shown in Figure 6. But in this case, the energy gap only shows a slow oscillation with its frequency at $\left(1.5\gamma+\gamma^2/\sqrt{3}\right)/\pi$, which is also well consistent with the result of FFA.

In the end, we should emphasize that the bond changes due to the curvature effect [23,24] was not included in our analytical formula, making our analytical results independent of the tube radius. In order to demonstrate the utility of our theoretical formula, we have made the

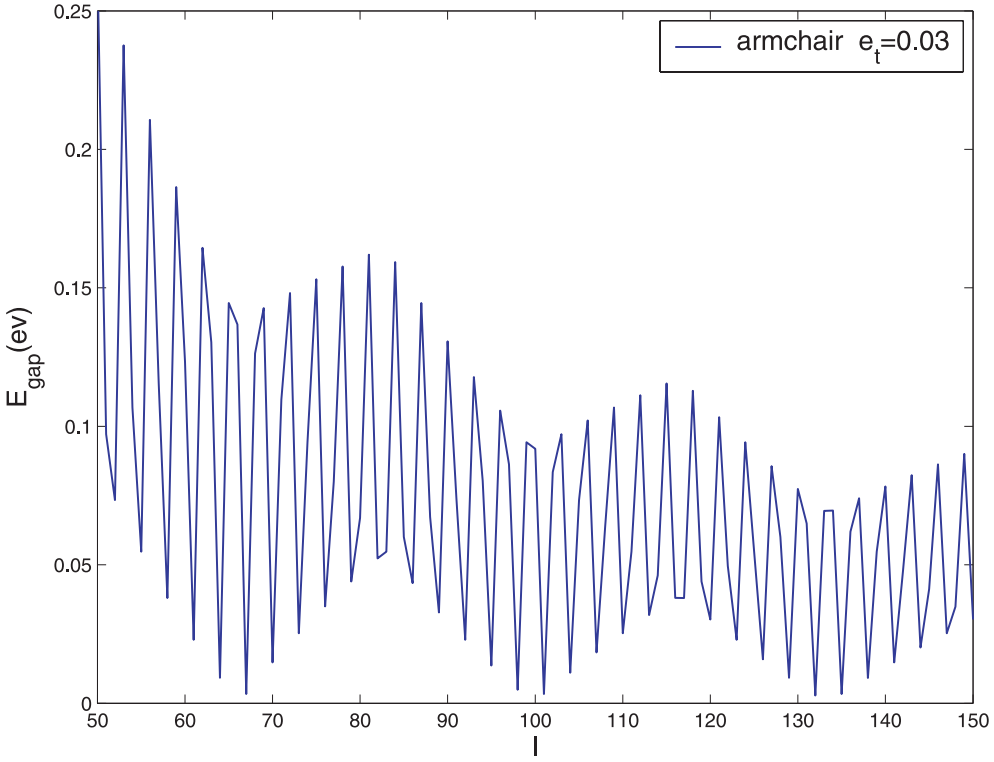


**Fig. 4.** Energy gap versus tube length of elongated finite-length armchair tubes.

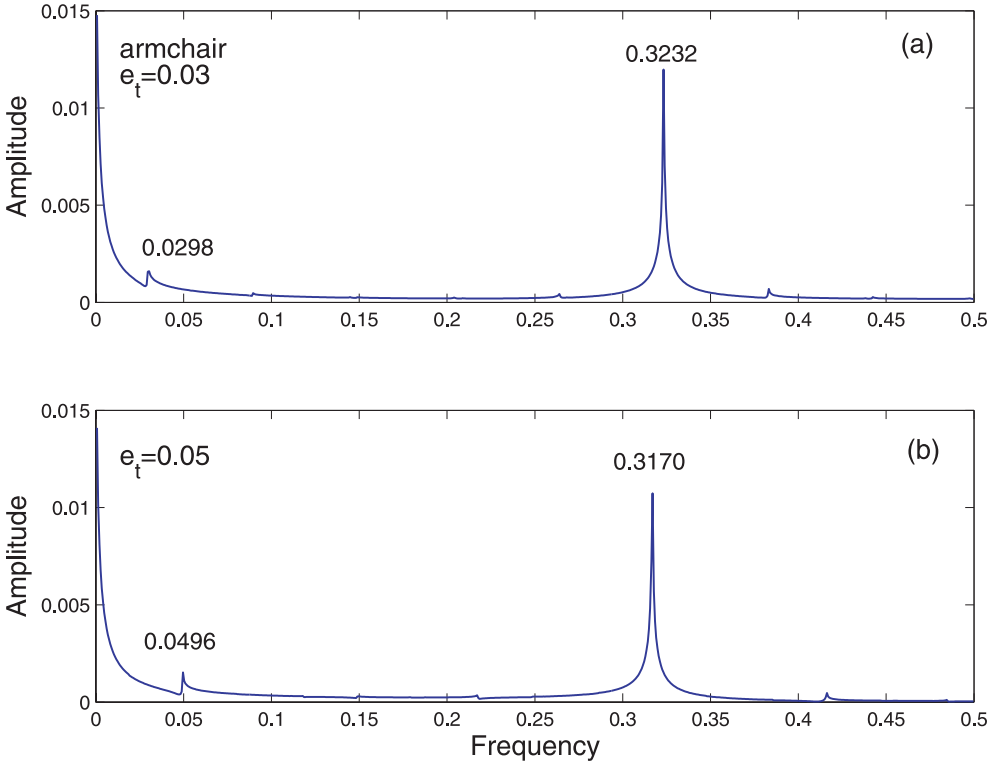


**Fig. 5.** The Fourier Frequency Analysis (FFA) of the energy gap versus tube length of elongated finite-length armchair tubes $e_t = 0.03$ (a) and $e_t = 0.05$ (b).

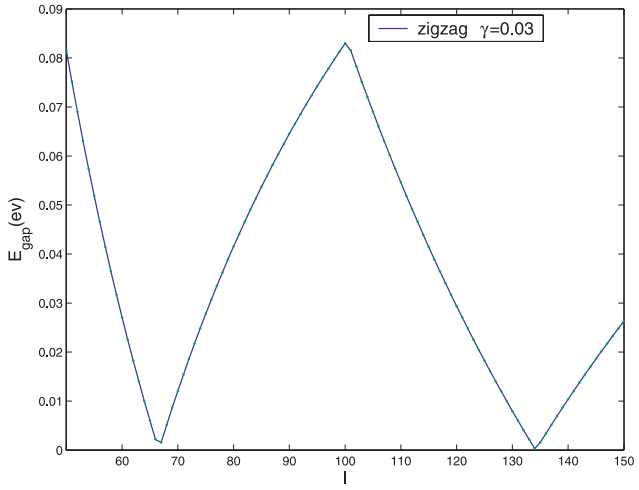


**Fig. 6.** Energy gap versus tube length of finite-length metallic zigzag tubes under torsional strain.

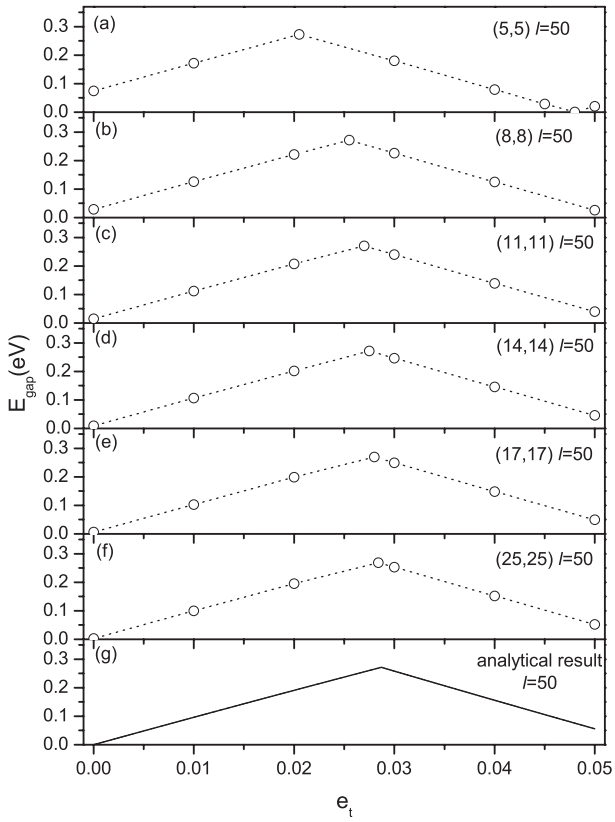


**Fig. 7.** The numerical results of energy gap versus uniaxial strain for different armchair tubes with fixed length $l = 50$. (a–f) correspond to (5, 5), (8, 8), (11, 11), (14, 14), (17, 17) and (25, 25) tubes, respectively. (g) The analytical result for armchair tube with $l = 50$.

numerical calculations in the pi-orbital nearest neighbor Hamiltonian on the energy gap versus uniaxial strain for armchair tubes of (5, 5), (8, 8), (11, 11), (14, 14), (17, 17) and (25, 25) with fixed length $l = 50$ by taking into account the curvature effects through a dependence of the hopping integral on the tube radius (Harrison relation [23]), whose results are shown in Figure 7a−f. It is found that, with increasing the tube diameter, our results will converge rapidly towards the analytical one (shown in Fig. 7g) obtained from equation (8), indicating that our analytical formula is valid for large diameter.

In summary, it is shown that the electronic properties of metallic CNTs are very sensitive to both of the applied strain and tube length. If we fix one of them and change another, the metallic CNTs will show oscillations of the energy gap and a metal-semiconductor transition will occur periodically, which could be used as a new experimental tool to precisely measure the nano-scale mechanical deformation degree, and used in future nano-electromechanical devices.

This work was supported by the Natural Science Foundation of China under Grant No.10474035, No. A040108 and No. 90103038.

## References

1. S. Iijima, Nature (London) **354**, 56 (1994)
2. C. Dekker, Phys. Today **52**, 22 (1999)
3. J.W. Mintmire, B.I. Dunlap, C.T. White, Phys. Rev. Lett. **68**, 631 (1992); N. Hamada, S.-I. Sawada, A. Oshiyama, Phys. Rev. Lett. **68**, 1579 (1992)
4. R. Saito, M. Fujita, G. Dresselhaus, M.S. Dresselhaus, Appl. Phys. Lett. **60**, 2204 (1992)
5. J.W.G. Wildöer, L.C. Venema, A.G. Rinzler, R.E. Smalley, C. Dekker, Nature (London) **391**, 59 (1998)
6. T.W. Odom, J.-L. Huang, P. Kim, C.M. Lieber, Nature (London) **391**, 62 (1998)
7. T. Hertel, R. Martel, Ph. Avouris, J. Phys. Chem. B **102**, 910 (1998)
8. T. Hertel, R. Walkup, Ph. Avouris, Phys. Rev. B **58**, 13870 (1998)
9. W. Thomas et al., Appl. Phys. Lett. **76**, 2414 (2000)
10. W. Clauss, D.J. Bergeron, A.T. Johnson, Phys. Rev. B **58**, R4266 (1998)
11. R. Heyd, A. Charlier, E. McRae, Phys. Rev. B **55**, 6820 (1997)
12. D.W. Brenner, J.D. Schall, J.P. Mewlkill, D.A. shenderova, S.B. Sinnott, Interplanet. Soc. **51**, 137 (1998)
13. C.L. Kane, E.J. Mele, Phys. Rev. Lett. **78**, 1932 (1997)
14. L. Yang, M.P. Anantram, J. Han, J.P. Lu, Phys. Rev. B **60**, 13874 (1999)
15. L. Yang, J. Han, Phys. Rev. Lett. **85**, 154 (2000)
16. L.C. Venema, J.W.G. Wildöer, H.L.J. Temminck Tuinstra, C. Dekker, A.G. Rinzler, R.E. Smalley, Appl. Phys. Lett. **71**, 2629 (1997)
17. M. Bockrath, D.H. Cobden, P.L. McEuen, N.G. Chopra, A. Zettl, A. Thess, R.E. Smalley, Science **275**, 1992 (1997)
18. S.J. Tans, M.H. Devoret, H. Dai, A. Thess, R.E. Smalley, L.J. Geerligs, C. Dekker, Nature (London) **384**, 474 (1997)
19. J. Jiang, J. Dong, D.Y. Xing, Phys. Rev. B **65**, 245418 (2002)
20. A. Rubio, D.S. Portal, E. Artacho, P. Ordejön, J.S. Soler, Phys. Rev. Lett. **82**, 3520 (1999)
21. T. Ito, K. Nishidate, M. Baba, M. Hasegawa, Surface Science **514**, 222 (2002)
22. S. Ogata, Y. Shibutani, Phys. Rev. B **68**, 165409 (2003)
23. W.A. Harrison, *Electronic Structure and the Properties of Solids* (Dover, New York, 1989)
24. A. Kleiner, S. Eggert, Phys. Rev. B **64**, 113402 (2001)